Deposition of Copper Phthalocyanine Films by Glow-Discharge-Induced Sublimation

Gianluigi Maggioni,*[,†,§] Alberto Quaranta,[†,§] Sara Carturan,[†,§] Alessandro Patelli,[||] Michele Tonezzer,[†,§] Riccardo Ceccato,[§] and Gianantonio Della Mea[†,§]

University of Padua c/o Istituto Nazionale di Fisica Nucleare, Laboratori Nazionali di Legnaro, Viale dell'Università 2, 35020 Legnaro, Padua, Italy, Department of Materials Engineering and Industrial Technologies, University of Trento, Via Mesiano 77, 38050 Povo, Trento, Italy, and Department of Electronics and Informatics, University of Padua, Via Gradenigo 6A, 35131 Padua, Italy

Received August 5, 2004. Revised Manuscript Received January 18, 2005

Copper phthalocyanine (CuPc) thin films have been deposited by a recently developed plasma-based method named glow-discharge-induced sublimation (GDS). The deposition of CuPc films has also been obtained by vacuum evaporation (VE) and the comparison of the two methods shows important structural differences. FT-IR and ion beam analyses (RBS-ERDA) show that the GDS-deposited films mainly consist of integer CuPc molecules, but at increasing deposition time the incorporation of damaged molecules becomes important. X-ray diffraction, FT-IR spectroscopy, and UV−vis analysis are used to study the microstructure of the CuPc films and point out that while the VE films consist of only α crystallites, a more disordered structure with the presence of both α and β polymorphs characterizes the GDS films. The latter films are also much more porous as shown by nitrogen physisorption measurements and SEM. Thermal treatments of the GDS films determine a decrease of the structural disorder at 250 °C and the complete transformation to the β polymorph at 290 °C.

1. Introduction

Despite the prolonged studies and applications of metal phthalocyanines (MPcs) during the last forty years, the scientific research on these organic semiconductors is still vivid owing to their unique properties, such as thermal stability, chemical inertness, and biocompatibility. MPcs are thus interesting for several applications, including chemical sensing,[1] photoconducting agents,[2] photovoltaic cell elements,[3] nonlinear optics,[4] and electrocatalysis.[5] In the gas-sensing field, MPcs are mainly used as electrical gas sensors, because of the conductivity changes induced by the adsorption of oxidizing or reducing gases such as NO_x, halogens, and ammonia. Detection of NO_2 gas down to 25 ppb concentration by means of a lead phthalocyanine film has been attained.[6] Recently, MPcs have also been successfully tested as opto-sensing materials for the detection of volatile organic compounds (VOCs).[7]

The classical deposition methods of thin organic films such as spin coating, dip coating, and the sol−gel method cannot be easily applied to the production of MPc coatings owing to the low solubility of these compounds in organic solvents, inaccurate thickness homogeneity control, and solvent retention. The solubility of MPcs can be enhanced by adding substituent groups which promote the film adhesion to the chosen substrate, but the complexity of the chemical synthesis as well as the related cost will increase. These drawbacks are avoided by using high-vacuum evaporation, which has become the most widely used technique for the deposition of MPc films. It is well-known that phthalocyanine films can feature different crystalline forms, including α, β, γ, and x polymorphs.[8,9] For copper phthalocyanine (CuPc) films, the most common polymorphs are the metastable α and the stable β. CuPc films evaporated at room temperature, at a pressure of less than 10^3 Pa, usually consist of α-phase crystallites. At higher deposition pressures or at substrate temperatures above 210 °C, the β-phase is obtained.[10] Moreover, α-phase crystallites undergo a complete transformation into β-phase after annealing at temperatures higher than 250 °C.[10,11] The two polymorphs, which have different electrical resistivity, packing density, and gas sensitivity, are usually identified by their characteristic X-ray patterns and by peculiar FT-IR and UV−vis spectroscopic features.[12]

* To whom correspondence should be addressed. E-mail: maggioni@lnl.infn.it.
† Istituto Nazionale di Fisica Nucleare.
§ Department of Materials Engineering and Industrial Technologies, University of Trento.
|| Department of Electronics and Informatics, University of Padua.

(1) Snow, A. W.; Barger, W. R. *Phthalocyanines: properties and applications*; Leznoff, C. C., Lever, A. B. P., Eds.; VCH Publishers: New York, 1989; Vol. 1, p 341.
(2) Law, K.-Y. *Chem. Rev.* **1993**, *93*, 449.
(3) (a) Wöhrle, D., Kreienhoop, L., Schlettwein, D. *Phthalocyanines: properties and applications*; Leznoff, C. C.; Lever, A. B. P., Eds.; VCH Publishers: New York, 1996; Vol. 4, p 219. (b) Anthopoulos, T. D.; Shafai, T. S. *Thin Solid Films* **2003**, *441*, 207.
(4) de la Torre, G.; Vazquez, P.; Agullo-Lopez, F.; Torres, T. *J. Mater. Chem.* **1998**, *8*, 1671.
(5) Böttger, B.; Schindewolf, U.; Avila, J. L.; Rodriguez-Amaro, R. *J. Electroanal. Chem.* **1997**, *432*, 139.
(6) Temofonte, T. A.; Schoch, K. F. *J. Appl. Phys.* **1989**, *65*, 1350.
(7) Spadavecchia, J.; Ciccarella, G.; Vasapollo, G.; Siciliano, P.; Rella, R. *Sens. Actuators, B* **2004**, *100*, 135.
(8) (a) Assour, J. M. *J. Phys. Chem.* **1965**, *69*, 2295. (b) Ebert, A. A., Jr.; Gottlieb, H. B. *J. Am. Chem. Soc.* **1952**, *74*, 2806.
(9) Sharp, J. H.; Abkowitz, M. *J. Phys. Chem.* **1973**, *77*, 477.
(10) Berger, O.; Fischer, W.-J.; Adolphi, B.; Tierbach, S.; Melev, V.; Schreiber, J. *J. Mater. Sci.: Mater. Electron.* **2000**, *331*, 11.
(11) Hassan, A. K.; Gould, R. D. *Phys. Status Solidi A* **1992**, *91*, 132.

10.1021/cm0487122 CCC: $30.25
Published on Web 03/12/2005

Plasma-based methods have also been reported to succeed in depositing MPc films: Kurosawa et al.[13] performed the deposition of plasma-polymerized copper phthalocyanine (pp-CuPc) thin films and tested the gas-sensing properties of pp-CuPc-coated piezoelectric quartz crystals. On the other hand, the activation of CuPc molecules during the evaporation process by means of a weakly ionized plasma was reported to be very effective in tailoring the film properties: an improvement of the mechanical properties and chemical resistance of the CuPc films was obtained without jeopardizing their gas-sensing features.[14]

A plasma-based technique has been lately developed for the deposition of thin organic coatings.[15,16] This method is based on the use of a weakly ionized glow discharge produced in a standard radio frequency magnetron sputtering equipment. Low-energy ($E < 1$ keV) noble gas (He, Ar,...) ions impinge on solid organic powder leading to the sublimation of the organic molecules and to their condensation onto the substrate. A very similar method had been applied by Sugimoto et al.[17] for the deposition of amino acid films, which were used for the detection of VOCs.[18]

The present work reports the deposition of CuPc films by means of this plasma-based technique, named glow-discharge-induced sublimation (GDS). To the best knowledge of the authors, this is the first time that CuPc films have been deposited by using glow-discharge-induced sublimation (GDS), which is an only recently developed deposition process. For this reason, a detailed characterization of the properties of the deposited films was necessary and has been partially carried out in this work, focusing the attention mainly on the microstructure which has been extensively investigated by many authors in the case of the evaporated films. Previous work on the GDS deposition of aromatic compounds such as polyimide precursor monomers[19] and 3-hydroxyflavone[16] pointed out the molecular damage induced by the ion bombardment and the partial retention of damaged molecules in the deposited films. Although the high rigidity of the CuPc molecule and the lack of labile substituent groups should ensure a better resistance to the ion-induced damage as compared to monomers and 3-hydroxyflavone, a study of the molecular damage is necessary taking into account the complexity of CuPc molecular structure and its very high sublimation temperature which hinders the sublimation of CuPc molecules thus promoting their ion-induced damage.

The sublimation of the CuPc molecules has been studied by measuring the deposition rate using a quartz crystal microbalance. To compare the physical properties of the GDS films with samples produced by a standard vacuum evaporation (VE) technique, CuPc films have been furthermore evaporated at different substrate temperatures. Rutherford backscattering spectrometry (RBS) and elastic recoil detection analysis (ERDA) have been used to determine the film composition. Particular attention has been paid to the study of the structure and morphology of the deposited films, which can affect their gas-sensing features, as previously observed in evaporated films.[20,21] Dogo et al.[20] showed that the electrical conductivity of α and β polymorphs of MPc films as well as their temperature of maximum conductivity is very different. Collins and Mohammed[21] reported a much higher sensitivity to ammonia for β-phase ZnPc films than for the α-phase ones. However, according to Dogo et al.[20] and Berger et al.,[10] although the correlation between the film structure and the gas response of MPc films is well acknowledged, it still is not completely understood. Three complementary techniques have been used to study the chemical structure of the deposited films, in compliance with Debe et al.:[12] X-ray diffraction (XRD), FT-IR analysis, and UV−vis absorption. The film morphology has been investigated by scanning electron microscopy (SEM). Nitrogen physisorption measurements have been used to determine the free surface area and the pore size distribution in the deposited films.

To highlight the different structural features of the GDS deposited films with respect to the evaporated samples, the evolution of the structure and morphology after thermal treatment at different temperatures has been studied for both sets of samples. The study of the thermal evolution of the physical properties of CuPc films and, in particular, of the α to β transition temperature is also important taking into account that the working temperature of these films in electrical gas-sensing applications can be up to 200 °C.[20]

2. Experimental Section

The experimental setup used for the deposition of CuPc films consisted of a vacuum chamber evacuated by a turbomolecular pump to a base pressure of 10^{-4} Pa. The glow discharge was sustained by a 1-in. cylindrical magnetron sputtering source connected to a radio frequency power generator (600 W, 13.56 MHz) through a matching box. The CuPc powder (750 mg, 99.5% purity, Acros Organics) was put on the surface of an aluminum target and placed on the sputtering source. The glow discharge feed gas was argon (99.9999%), whose pressure inside the chamber was measured through a capacitance gauge. Typical values of rf power, target DC self-bias, and working pressure were in the ranges 10−20 W, −20 to −300 V, and 5.00 ± 0.05 Pa, respectively. The CuPc films were deposited on two substrates simultaneously, that is, P-doped (100) silicon wafer 350-μm-thick lapped on both faces (Atomergic Chemetals Inc.) and quartz glass slide (Heraeus Quarzglas GmbH & Co). The substrates were mounted on a sample holder placed 7 cm above the source.

(12) Debe, M. K.; Kam, K. K. *Thin Solid Films* **1990**, *186*, 289.
(13) (a) Kurosawa, S.; Kamo, N.; Matsui, D.; Kobatake, Y. *Anal. Chem.* **1990**, *62*, 353. (b) Kurosawa, S.; Arimura, T.; Tamura, M.; Shibakami, M.; Sekiya, A.; Kamo, N. *Jpn. J. Appl. Phys.* **1995**, *34*, 3658.
(14) Choi, C.-G.; Lee, S.; Lee, W.-J. *Sens. Actuators, B* **1996**, *32*, 77.
(15) Maggioni, G.; Carturan, S.; Rigato, V.; Della Mea, G. *Surf. Coat. Technol.* **2001**, *142−144*, 156.
(16) Maggioni, G.; Carturan, S.; Quaranta, A.; Patelli, A.; Della Mea, G. *Chem. Mater.* **2002**, *14*, 4790.
(17) Sugimoto, I.; Nakamura, M.; Kuwano, H. *Anal. Chem.* **1994**, *66*, 4316.
(18) (a) Sugimoto, I.; Nakamura, M.; Kuwano, H. *Sens. Actuators, B* **1996**, *37*, 163. (b) Sugimoto, I.; Nakamura, M.; Kasai, N.; Katoh, T. *Polymer* **2000**, *41*, 511.
(19) Maggioni, G.; Quaranta, A.; Negro, E.; Carturan, S.; Della Mea, G. *Chem. Mater.* **2004**, *16*, 2394.
(20) (a) Dogo, S.; Germain, J. P.; Maleysson, C.; Pauly, A. *Sens. Actuators, B* **1992**, *8*, 257. (b) Dogo, S.; Germain, J. P.; Maleysson, C.; Pauly, A. *Thin Solid Films* **1992**, *219*, 251.
(21) (a) Sadaoka, Y.; Jones, T. A.; Revell, G. S.; Gopel, W. *J. Mater. Sci.* **1990**, *25*, 5257. (b) Sadaoka, Y.; Matsuguchi, M.; Sakai, Y.; Mori, Y.; Göpel, W. *Sens. Actuators, B* **1991**, *4*, 495. (c) Hsieh, J. C.; Liu, C. J.; Ju, Y. H. *Thin Solid Films* **1998**, *322*, 98. (d) Collins, R. A.; Mohammed, K. A. *J. Phys. D: Appl. Phys.* **1988**, *21*, 154.

The vacuum chamber used for the evaporation of CuPc coatings has been described elsewhere.[22] The films were evaporated on substrates both kept at room temperature (RTVE films) and cooled to −60 °C (LTVE films). A quartz crystal microbalance was used to measure in real time the deposition rate of the organic layer in both deposition setups. When measuring the GDS deposition rate, the sample holder was removed and the microbalance replaced the sample holder. The GDS deposition rate was recorded every 10 s. The thickness of evaporated and GDS-deposited films ranged from 1 to 2 μm.

The measurement of the film composition was performed by ion beam analyses using 2.2 $^4He^+$ beam at the Van de Graaf accelerator at the Laboratori Nazionali di Legnaro. In particular, copper, nitrogen, and carbon concentration was determined by Rutherford backscattering spectrometry (RBS) at the scattering angle of 160°, whereas hydrogen concentration was measured by elastic recoil detection analysis (ERDA) at a recoil angle of 30° and at grazing incidence of 15°. Ion beam analyses were performed on a CuPc coating deposited on a graphite substrate. Graphite was chosen to obtain well-isolated carbon and nitrogen peaks. To separate the film carbon peak from the substrate carbon, an aluminum interlayer was deposited on the graphite before the CuPc coating deposition.

The surface morphology of the samples was investigated with a scanning electron microscope (SEM, Philips XL-30). Structural analyses were carried out by means of X-ray diffraction (XRD) using a Rigaku D-Max III diffractometer. For XRD measurements of thin films deposited on silica substrates, an asymmetric scattering configuration was adopted with an incidence angle (θ) of 1°, a scan interval of $3° < 2\theta < 40°$, and 60 s of counting time. Powder spectra were collected within the same scan interval but with 5 s of counting time.

FT-IR spectra of the samples were recorded in the 4000−400 cm^{-1} range using a Jasco FT-IR 660 Plus spectrometer with a resolution of 4 cm^{-1}. The sample cell and the interferometer were evacuated to remove the absorption peaks of water and atmospheric gases.

UV−visible absorption measurements were performed in the 200−800 nm range using a Jasco V-570 dual-beam spectrophotometer. The spectra were recorded with a resolution of 2 nm.

Nitrogen physisorption experiments were carried out at 77 K on an ASAP 2010 Micromeritics sorptometer. CuPc powders obtained by scraping off VE and GDS films were degassed below 1.3 Pa at 25 °C. The specific surface area (SSA) was calculated by the BET equation in the interval $0.05 \le p/p_0 \le 0.33$ with a least-squares fit of 0.998. The BJH method was applied both on the adsorption and desorption branches to estimate the pore size distribution.

3. Results and Discussion

3.1 Physical and Morphological Properties of As-Deposited Samples. Figure 1 shows the deposition rate of GDS-deposited CuPc films as a function of deposition time and rf power in the range 10−20 W: the starting deposition rate increases with the rf power owing to the increase of the ion current density on the target surface. However, for all three power values, the rate appears to be quite irregular as compared to the trend of other previously studied organic compounds, such as polyimide precursor monomers,[19] where a monotonic decrease was observed as a function of deposition time. In that case, the decrease was due to the slow ion-bombardment-induced formation of a damaged surface layer on the organic powder, which progressively hindered the sublimation of integer molecules. In the CuPc deposition, the formation of the damaged layer is much quicker because of the high heat of sublimation of this compound. The formation of the damaged layer is highlighted by a color changing of the surface powder from blue to black after the deposition has been completed. FT-IR analysis of the black powder shows the lack of any feature in the whole range (4000−400 cm^{-1}). The damaged layer inhibits the sublimation of the underlying CuPc molecules; the heat accumulated during the ion bombardment produces a remarkable increase in the pressure below the layer until the latter breaks thus producing the sudden, massive sublimation of nano- and microaggregates of CuPc molecules. This effect is depicted by the appearance of the prominent peaks in the deposition rate graph (Figure 1). A SEM inspection confirms the presence of these aggregates on the film surface. The appearance of the peaks is not strictly linked to the rf power, as shown by the very limited number of peaks at 15 W, but it is thought to depend on the powder morphology and granulometry. The aggregate emission does not occur in the CuPc evaporation and the VE film surface appears flat and homogeneous.

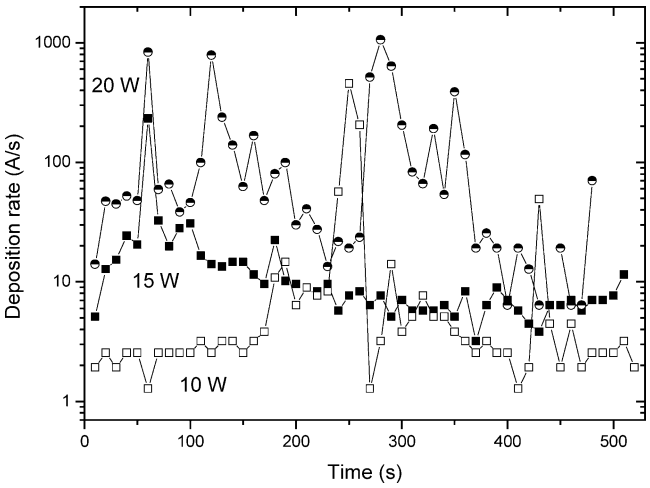

Figure 1. GDS deposition rate of copper phthalocyanine as a function of the deposition time at three different rf powers.

Whereas the presence of grains on the GDS film surface would be deemed undesirable in most cases, it is regarded positively in this context in view of the application of these coatings in gas sensors, since it increases the average film porosity (see below). As a matter of fact, micro- and nanostructured SnO_2-based gas sensors have recently been shown to feature a very high sensitivity.[23] On the other hand, the pronounced spikes of the deposition rate make the in-situ film thickness measurement necessary to ensure the complete control of the deposition process.

FT-IR spectra of a vacuum-evaporated film deposited at room temperature (RTVE) and of GDS films deposited at 20 W for different times (from 175 to 1150 s) are reported in Figure 2: a comparison between these spectra points out

(22) Maggioni, G.; Carturan, S.; Boscarino, D.; Della Mea, G.; Pieri, U. *Mater. Lett.* **1997**, *32*, 147.

(23) (a) Comini, E.; Ferroni, M.; Guidi, V.; Faglia, G.; Martinelli, G.; Sberveglieri, G. *Sens. Actuators, B* **2002**, *84*, 26. (b) Shi, L.; Hasegawa, Y.; Katsube, T.; Onoue, K.; Nakamura, K. *Sens. Actuators, B* **2004**, *99*, 361.

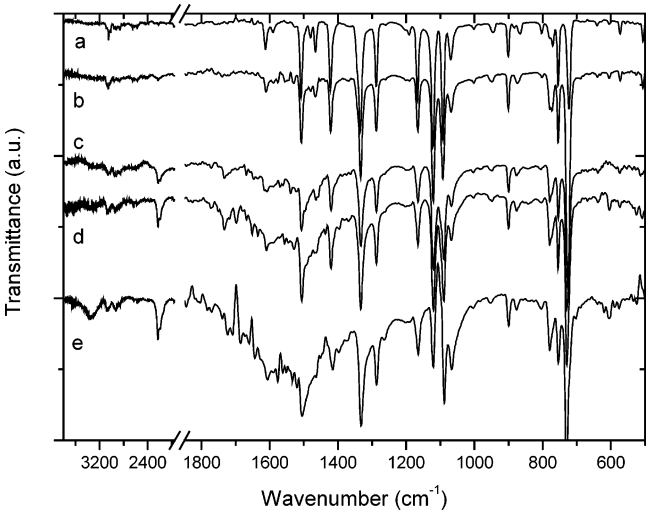

Figure 2. FT-IR spectra of RTVE film (a) and GDS films deposited for (b) 175 s, (c) 340 s, (d) 480 s, and (e) 1150 s.

the evolution of the GDS film composition as a function of deposition time. The spectrum of the sample deposited for 175 s is very similar to the RTVE film spectrum: all the main peaks of CuPc molecule can be identified. This finding together with the lack of any extraneous feature in the GDS sample spectrum shows that this film is mainly made of integer CuPc molecules. On the other hand, the appearance of new features is observed at increasing deposition time: a peak centered at 2230 cm^{-1}, which is ascribed to the C≡N stretching, a N−H stretching band at 3350 cm^{-1}, and a broad band between 1700 and 1250 cm^{-1}. According to Xu et al.,[24] this last band, which had already been observed in plasma-polymerized CuPc films,[13] can arise from the formation of a structure that is similar to amorphous graphite. However, the appearance of all these new spectral features can only be related to the incorporation of damaged molecules in the deposited films.

The negligible incorporation of damaged molecules in the GDS film for low deposition times is confirmed by the ion beam analysis of the sample deposited for 175 s (Figure 3). The atomic ratios between the elements of the GDS film (Cu, N, and H) and carbon, as calculated by RBS/ERDA analyses, are 0.031 ± 0.002, 0.25 ± 0.002, and 0.50 ± 0.07, respectively. Although the relatively high experimental error on the hydrogen determination must be taken into account, these values coincide with the theoretical atomic ratios.

The structure of the deposited films has been studied by X-ray diffraction, FT-IR, and UV−vis analyses. Figure 4 shows the XRD spectra of β-phase and α-phase CuPc powders, RTVE and low-temperature-evaporated (LTVE) films, and both GDS film and powder. The GDS film has been deposited for 175 s. The α-phase and GDS powders have been obtained by scraping off the RTVE film and the GDS film, respectively. The X-ray diffraction spectra of the as-deposited VE films are similar to those reported in the literature for RT-evaporated CuPc.[10,25] They exhibit some

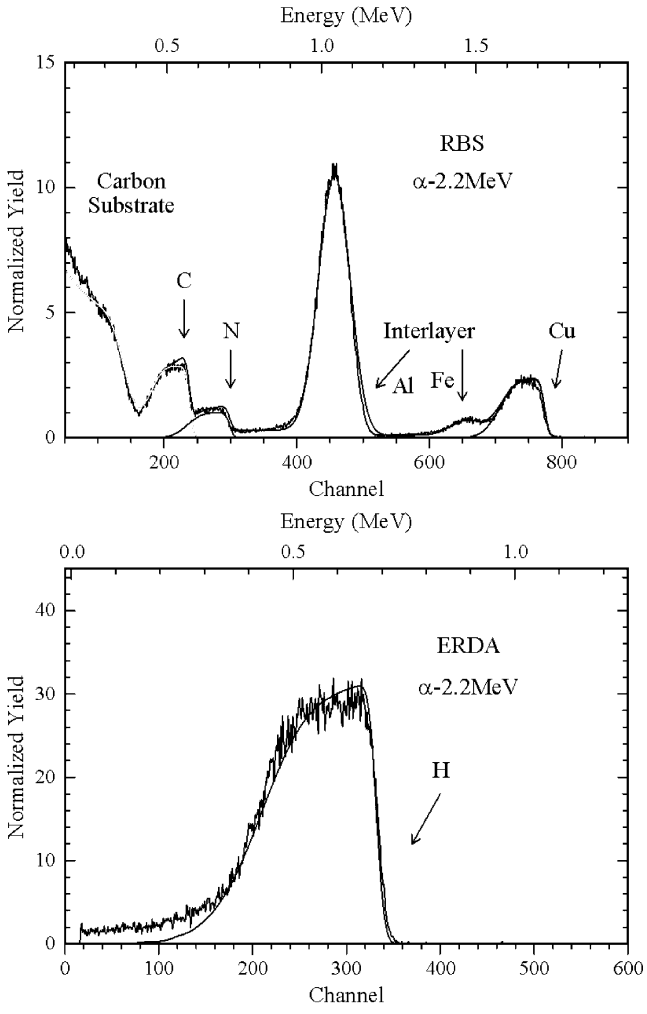

Figure 3. RBS and ERDA spectra of CuPc coating deposited on aluminum-coated graphite substrate. The Fe peak is due to an aluminum interlayer contamination.

typical features of the α phase (JCPDS Card 6-0007), that is, two overlapped peaks at $d = 12.8$ Å (001) and $d = 12.2$ Å (110) and other less intense peaks at $d = 3.68$ Å (421), 3.49 Å (223), 3.40 Å (510), and 3.23 Å (520). The lack of the peaks appearing at about $d = 8.63$ Å (200) and $d = 5.49$ Å (310) in the spectrum of the α powder can be ascribed to the presence of preferentially oriented α crystallites.[25] This feature is particularly evident in the RTVE film, which shows a strong relative intensity of the (001) reflection together with a lower intensity of the (110) reflection. The average α crystallite size has been calculated by means of the Warren−Averbach method[26] and is 3 nm for the LTVE film and 12 nm for the RTVE film. On the other hand, the calculated crystallite size in the α powder is 5 nm, which means that the average size of the randomly oriented crystallites is smaller than that of the preferentially oriented crystallites.

As far as the GDS sample is concerned, its spectrum exhibits two weak reflections peaked at $d = 12.8$ and 9.6 Å. The latter, which is absent in all the α samples (powder and films), can be assigned to the (−102) reflection of the β polymorph (JCPDS 11-0893) and indicates the presence of

(24) Xu, D.; Xu, X. L.; Du, G. D.; Wang, R.; Zou, S. C.; Liu, X. H. *Nucl. Instrum. Methods B* **1993**, *80/81*, 1063.
(25) Resel, R.; Ottmar, M.; Hanack, M.; Keckes, J.; Leising, G. *J. Mater. Res.* **2000**, *15*, 934.
(26) Warren, B. E.; Averbach, B. L. *J. Appl. Phys.* **1950**, *21*, 595.

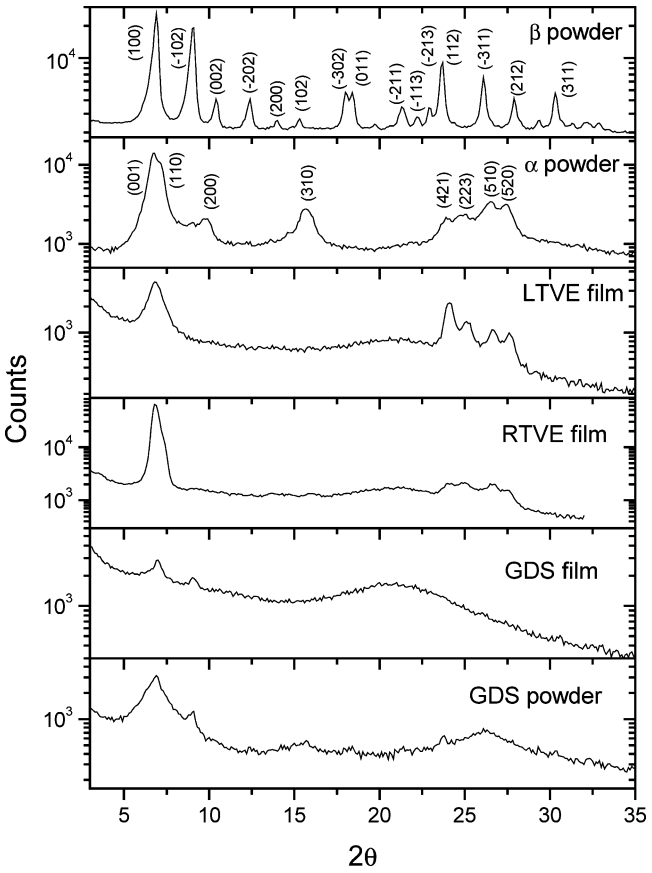

Figure 4. X-ray diffraction spectra of β, α, and GDS powders and of VE and GDS films.

β crystallites in the GDS film. On the other hand, the reflection peaked at $d = 12.8$ Å cannot be exclusively assigned either to the β(100) or to the α(001) and (110) reflections, but it derives from the overlapping of both contributions. As a matter of fact, the presence of both polymorphs in the GDS film is highlighted by the spectrum of the GDS powder in which several broad α and β reflections appear. The presence of both polymorphs makes the calculation of the average crystallite size of the GDS film particularly difficult: besides the reflection at $d = 12.8$ Å, the broad band between $2\theta = 23.5°$ and $2\theta = 28°$ derives from the overlapping of the α(421), (223), (510), and (520) reflections and of the β(−311) and (212) reflections. Moreover, the presence of residual strains between the crystallite planes, which determine a broadening of the X-ray peaks, cannot be ruled out, taking into account the very high GDS deposition rate that freezes the CuPc admolecules in their position when they impinge onto the substrate. For all these reasons, an unambiguous evaluation of the average crystallite size of the GDS film cannot be attained. However, the broadness of all the peaks appearing in the spectrum suggests the presence of high disorder in the GDS film with a broad distribution of crystallite size and lattice parameter.

The structure of the deposited films has also been studied by FT-IR analysis. It is well-known that the MPc α and β polymorphs are characterized by some selected IR peaks related to the short-range neighbor interactions.[27,11,28] The IR spectra (region 1190−700 cm^{-1}) of both as-deposited VE

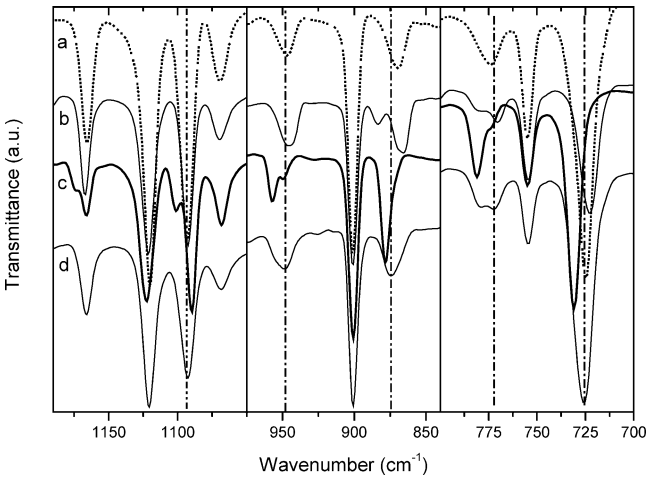

Figure 5. FT-IR spectra of (a) LTVE film; (b) RTVE film; (c) RTVE film treated at 290 °C; and (d) GDS film (regions: 1190−1050 cm^{-1}; 975−840 cm^{-1}; 800−700 cm^{-1}).

films, the RTVE film treated at 290 °C, and the GDS film are compared in Figure 5. According to Sidorov and Kotlyar,[27] the peculiar IR features of CuPc α and β polymorphs are (i) the out-of-plane hydrogen bending mode (γ(C−H)) peak at 722 cm^{-1} (α) and 730 cm^{-1} (β); (ii) the peak at 770 cm^{-1} (α) and at 780 cm^{-1} (β), which has been ascribed to a vibrational mode of the central part of the CuPc cycle;[29] (iii) the unresolved peaks at 864 and 870 cm^{-1} and the peak at 940 cm^{-1} (α) against the peaks at 877 and 957 cm^{-1} (β); and (iv) a peak at 1100 cm^{-1} and a shoulder at 1174 cm^{-1}, which are characteristic of the β polymorph. As to the reported spectra, the features of α polymorph are identified in the RTVE film and those of β polymorph in the RTVE film treated at 290 °C. On the other hand, some differences with respect to both polymorphs are found in the LTVE film, although this sample exhibits features closer to those of the α polymorph than to β. The main differences are that the γ(C−H) peak is centered at 725 cm^{-1} instead of 722 cm^{-1} and only one peak appears at 773 cm^{-1}; moreover, the α peak at 864 cm^{-1} lacks. Considering that XRD analysis of this sample points out the presence of only α crystallites, the findings of FT-IR analysis are partially unexpected and some doubts about the correlation between the position of the γ(C−H) peak and the crystalline structure arise. As previously highlighted by XRD analysis, the main differences between these two samples concern the preferential orientation (more pronounced in the RTVE sample) and the average crystallite size. As could be expected, the preferential orientation does not affect the IR features: in fact, the γ(C−H) peak of the α powder is centered at 722 cm^{-1}. On the other hand, the influence of the average crystallite size on the peak position appears to be more critical. As a matter of fact, a crystallite with a size of 5 nm contains nearly five molecular planes. Therefore, the amount of CuPc molecules, which lie on the crystallite surface and are thus more susceptible to the different chemical surroundings, is smaller than the amount of the core molecules surrounded by an unperturbed α phase environment. On the contrary, when

(27) Sidorov, A. N.; Kotlyar, I. P. *Opt. Spectrosc.* **1961**, *11*, 92.
(28) Sadaoka, Y.; Goepel, W.; Suhr, B.; Rager, A. *J. Mater. Sci. Lett.* **1990**, *1481*, 9.
(29) Shurvell, H. F.; Pinzuti, L. *Canad. J. Chem.* **1966**, *44*, 125.

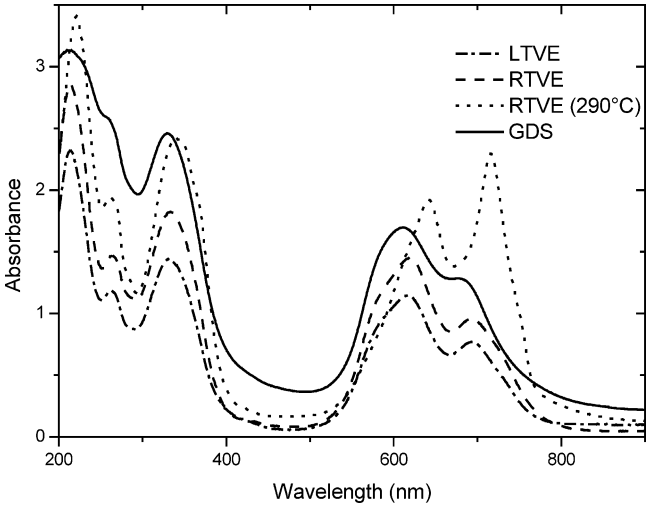

Figure 6. UV−vis absorption spectra of LTVE film (— - —), RTVE film (— —), RTVE film treated at 290 °C (- -), and GDS film (——).

the average size drops to 3 nm or less, the crystallite contains no more than three molecular planes so that the contribution of the surface CuPc molecules becomes important with respect to that of the core molecules and a perturbation of the IR features takes place.

As to the GDS sample, a clear assignation to a single phase cannot be done, but a mixture of both polymorphs is found and confirms the findings of the XRD analysis: as a matter of fact, the γ(C−H) peak is centered at 726 cm^{-1} and two peaks at 773 and 780 cm^{-1} overlap; another peak is centered at 875 cm^{-1} instead of either 870 cm^{-1} (α) or 877 cm^{-1} (β), and the peak at 949 cm^{-1} exhibits a weak shoulder at 957 cm^{-1} (β). On the other hand, the β features at 1100 and 1174 cm^{-1} cannot be identified. Taking into account the IR features of the LTVE film, the position of the γ(C−H) peak and the appearance of the peak at 773 cm^{-1} point at the presence of small α crystallites. However, the presence of bigger α crystallites cannot be ruled out, since the γ(C−H) peak at 726 cm^{-1} can also arise from the overlapping of two peaks centered at 730 and 722 cm^{-1}. In the latter case, the residual strains between the crystalline planes, whose presence has not been ruled out above, can give rise to the broadening of both peaks, which are the most sensitive to the surrounding environment, thus promoting their overlapping.

The study of the structure of the deposited films has been completed by measuring their UV−vis optical absorption. Since the thick films used for FT-IR and XRD gave rise to saturation, thinner VE films (only 100 nm) have been analyzed to point out the spectral features of the α and β polymorphs, as reported in the literature.[9,30]

Figure 6 shows the absorption spectra of both as-deposited VE films, the RTVE film treated at 290 °C, and the GDS film. All the samples exhibit two bands, that is, the Q-band between 500 and 800 nm and the B band (Soret band) between 200 and 400 nm.[9,30] Both as-deposited VE films present the typical features of the α polymorph: the Q-band is peaked at 619 and 693 nm and the B band at 214, 264 and 333 nm. For the RTVE film treated at 290 °C, the features of the β polymorph are identified: the Q-band peaks shift to 642 and 716 nm, while the high-wavelength B band peak is at 342 nm.

As far as the GDS film is concerned, its spectrum appears more similar to α phase than to β, because it exhibits a Q-band peaked at 613 and 680 nm and a B band at 211, 262, and 334 nm. In particular, the two peaks of the Q-band are broader than the corresponding ones in the VE samples: this could be due to both the higher disorder present in the GDS film and the presence of weak features of the β polymorph which overlap those of the α phase. The very disordered and porous structure of the GDS film, as highlighted by SEM (see Figure 7), also gives rise to the

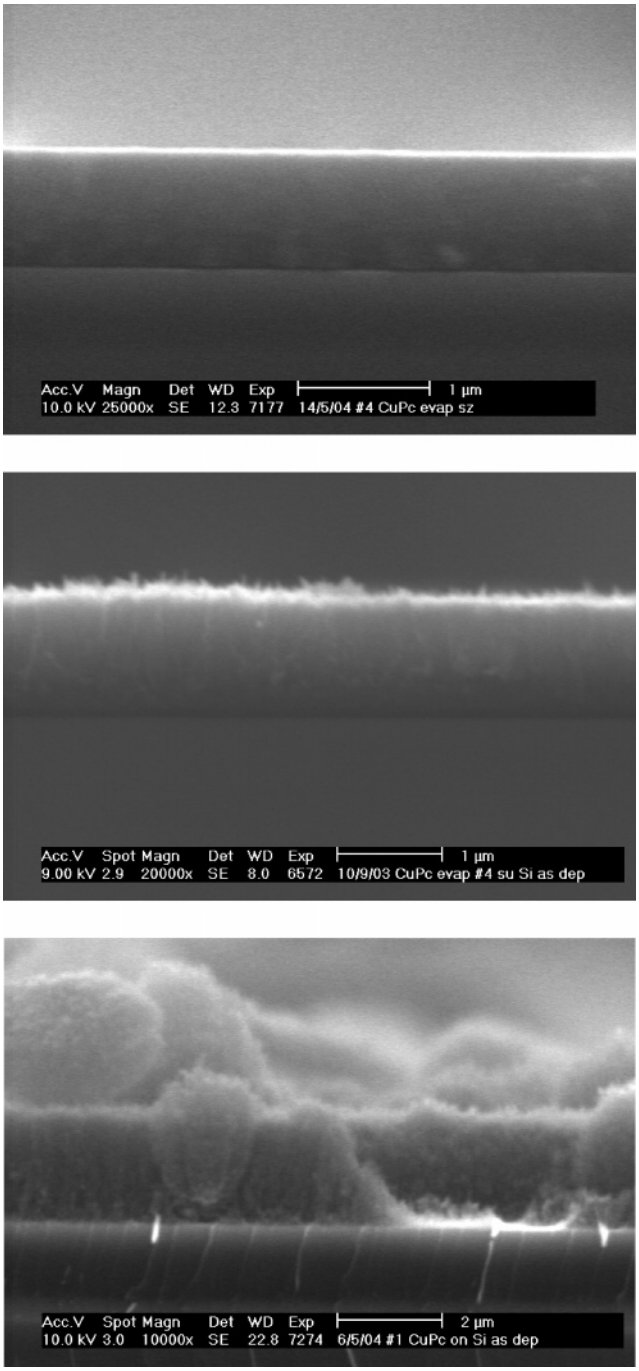

Figure 7. Cros-sectional SEM micrographs of LTVE film (upper), RTVE film (middle), and GDS film (lower).

(30) (a) Lucia, E. A.; Verderame, F. D. *J. Chem. Phys.* **1968**, *48*, 2674. (b) Harrison, S. E.; Ludewig, K. H. *J. Chem. Phys.* **1996**, *45*, 343.

background present in the whole absorption spectrum owing to the light scattering on the morphological inhomogeneities.

The lack of any absorption peak at 782 nm excludes the presence of the x polymorph, which is mostly characterized by this peculiar UV−vis feature.[9,12,31]

To sum up, the structural characterization of the GDS films demonstrates that these films mainly consist of a mixture of α and β crystallites, with a predominance of the α polymorph, as shown by UV−vis absorption spectra. The growth of this kind of structure is thought to be due mainly to two concomitant effects: first, the condensation of big amounts of CuPc molecules in a very short time, which takes place during the pronounced spikes of the GDS deposition rate, implies that the molecules are frozen in their positions and can neither move nor rotate to find a lower energy configuration. By this way, the residual crystalline strains probably arising during the film growth cannot be relaxed and remain in the film. The second effect involves the relatively high deposition pressure, which is nearly 4 orders of magnitude higher than the standard evaporation. The high pressure can give rise to the deposition of a mixture of both phases in agreement with the results of Griffiths and Walker as reported by Sharp and Abkowitz,[9] which found both polymorphs in films evaporated at pressures ranging from 10^{-2} to 10 Pa.

In addition to the peculiar structural characteristics, the GDS films feature a very different morphology with respect to the as-deposited VE films, as highlighted by cross-sectional SEM images in Figure 7 and by the heat treatments described below. In fact, while the VE films are relatively flat and compact, the GDS films are characterized by a rough structure with big grains (2 μm and more) and a high porosity inside and between the grains.

Nitrogen physisorption measurements confirm the higher porosity of the GDS film as compared to the RTVE sample. Physisorption curves of both samples show a type-IV isotherm (Figure 8). The hysteresis loop is actually less evident for the GDS film than that for the evaporated one, which shows the loop onset in the desorption branch at around 0.5 P/P_0. Specific surface area (SSA) values, calculated for the GDS film, are higher than those for the RTVE sample: in fact, RTVE film features 31 m^2/g against 155 m^2/g of the GDS film. The pore size distribution curve of the RTVE film, as obtained from the desorption branches, features a monomodal and sharp distribution centered at around 4 nm. By contrast, GDS film is characterized by a bimodal distribution with micropores (≈2 nm) and mesopores (>30 nm).

The high porosity of the GDS films, with respect to the VE samples, makes them very interesting for applications in the gas-sensing field.

3.2 Physical and Morphological Properties of Heat-Treated Samples. Figures 9−11 display the FT-IR and XRD spectra of the deposited samples before and after the thermal treatments at 250 °C and 290 °C for 14 h. Treatment time was chosen in compliance with Prabakaran et al.[32] to ensure

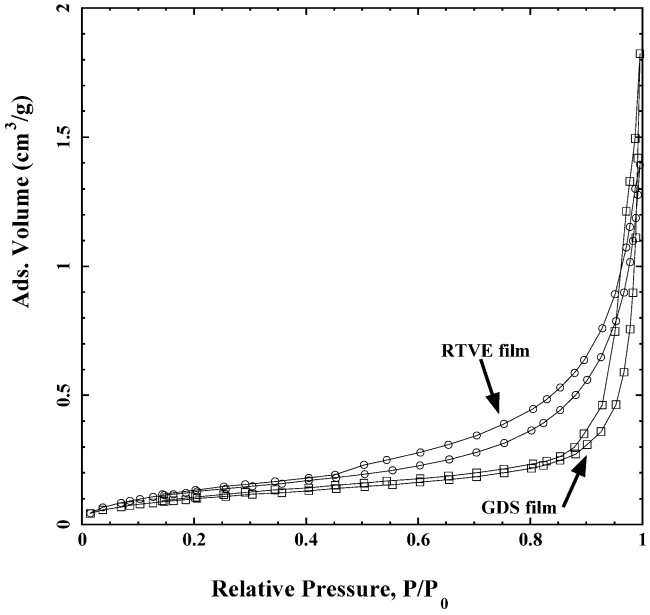

Figure 8. Nitrogen physisorption graphs of RTVE film (○) and GDS film (□).

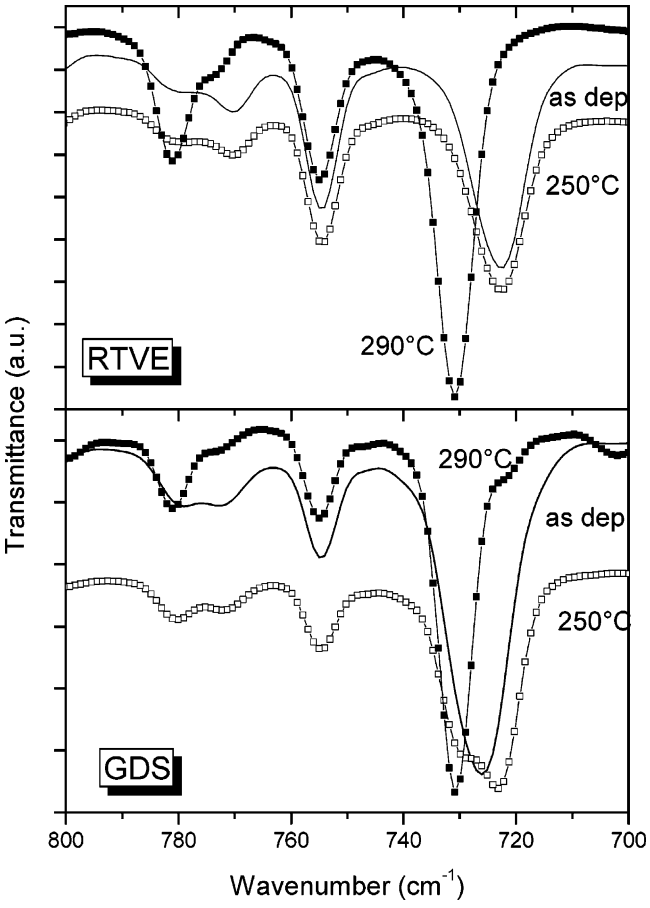

Figure 9. FT-IR spectra of thermally treated samples: VE films (upper) and GDS films (lower).

the completion of possible structural modifications (either phase transition or grain growth). After the treatment at 250 °C, the RTVE film consists of only α polymorph as shown by FT-IR and XRD analyses. Moreover, the increased intensity of the (110) and (001) reflections in the XRD spectrum with respect to the other reflections indicates the increase in the number of preferentially oriented α crystal-

(31) Meshkova, G. N.; Vartanyan, A. T.; Sidorov, A. N. *Opt. Spectrosc.* **1977**, *43*, 151.
(32) Prabakaran, R.; Kesavamoorthy, R.; Reddy, G. L. N.; Xavier, F. P. *Phys. Status Solidi B* **2002**, *229*, 1175.

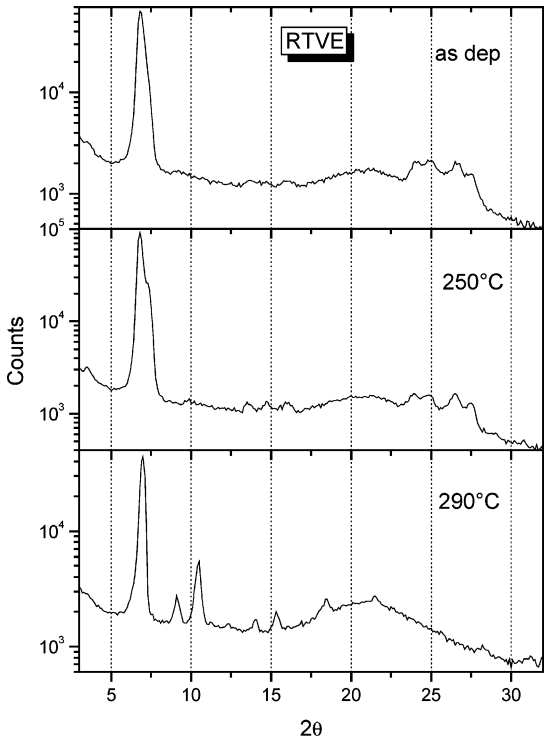

Figure 10. XRD spectra of RTVE samples as-deposited (upper), treated at 250 °C (middle), and treated at 290 °C (lower).

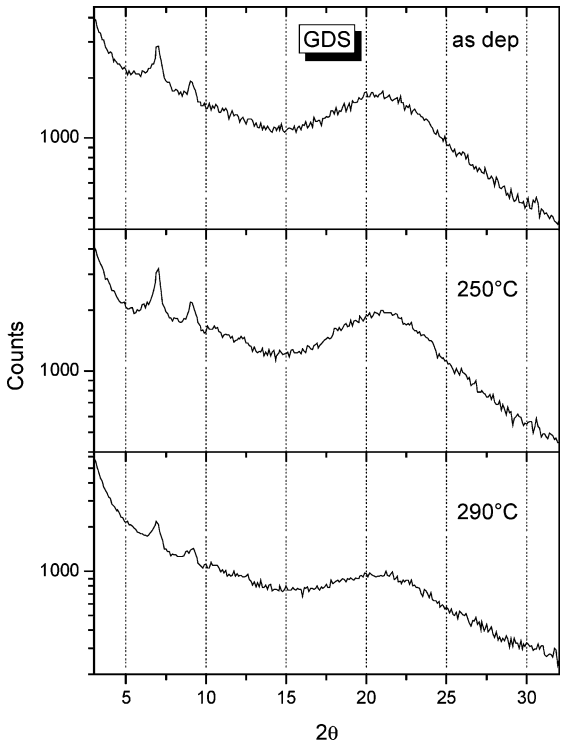

Figure 11. XRD spectra of GDS samples as-deposited (upper), treated at 250 °C (middle), and treated at 290 °C (lower).

lites. This suggests that the oriented crystallites act as nucleation centers to promote the growth of similarly oriented crystallites. The lack of any clear evidence of α to β transformation at this temperature by both FT-IR and XRD analyses is noteworthy. This finding seems to be in contrast with those of Berger et al.[10] (for CuPc) and Liu et al.[33] (for

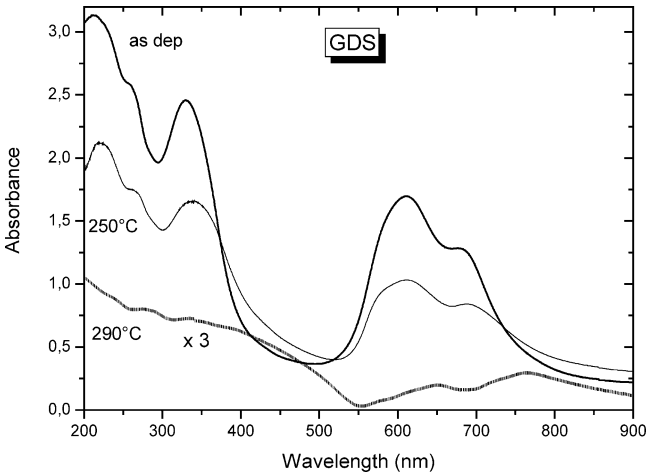

Figure 12. UV−vis spectra of thermally treated GDS films.

NiPc), who observed a partial transformation after only 1 h. Moreover, Hassan and Gould[11] found a partial α to β transformation after 3 h at 240 °C. The discrepancy can be overcome by assuming that the transformation trigger depends on the average size of the α crystallites: when the film is either completely amorphous or containing α crystallites with a size smaller than a threshold value, the transformation to β polymorph is promoted; otherwise, when the crystallites are bigger (as in the RTVE film), the only effect of the treatment is the growth of the α crystallites and a higher temperature is necessary to trigger the α to β transition (e.g., 290 °C). This hypothesis is confirmed by the behavior of the LTVE sample, whose structure is almost completely transformed to β polymorph after heating at 250 °C, as shown by FT-IR analysis (see Supporting Information). Moreover, a grain-size-induced structural phase transition was already observed in other systems such as nanocrystalline lead lanthanum titanate, which undergoes a transition from tetragonal to cubic phase at room temperature, when the grain size is smaller than 20 nm.[34]

After the treatment at 290 °C, the α to β transformation is completed, as pointed out by the shift of the γ(C−H) peak from 722 to 730 cm^{-1} and by the inversion of the intensity ratio between the peaks at 770 and 780 cm^{-1}. In the XRD spectrum, the transformation is confirmed by the disappearance of the α reflections and by the appearance of several reflections of the β polymorph. The low intensity of the β(−102) reflection as compared to (100), which on the other hand are comparable in the β powder spectrum, shows that the preferential orientation is preserved even after the thermal treatment. This could be expected because only a low amount of energy is necessary for the single molecules to form the nuclei of the β phase and to rearrange themselves into the new crystal lattice, if the β crystals grow maintaining the stacking axis in the same direction as the original α crystals.[10]

In the GDS samples, the treatment at 250 °C determines a splitting of the γ(C−H) peak at 726 cm^{-1} in two partially overlapped peaks centered at 729 and 722 cm^{-1} (Figure 9). These peaks are typical features of β polymorph and of big-sized α polymorph, respectively, as previously shown for

(33) Liu, C. J.; Shih, J. J.; Ju, Y. H. *Sens. Actuators, B* **2004**, *99*, 344.

(34) Zhou, Q. F.; Chan, H. L. W.; Zhang, Q. Q.; Choy, C. L. *J. Appl. Phys.* **2001**, *89*, 8121.

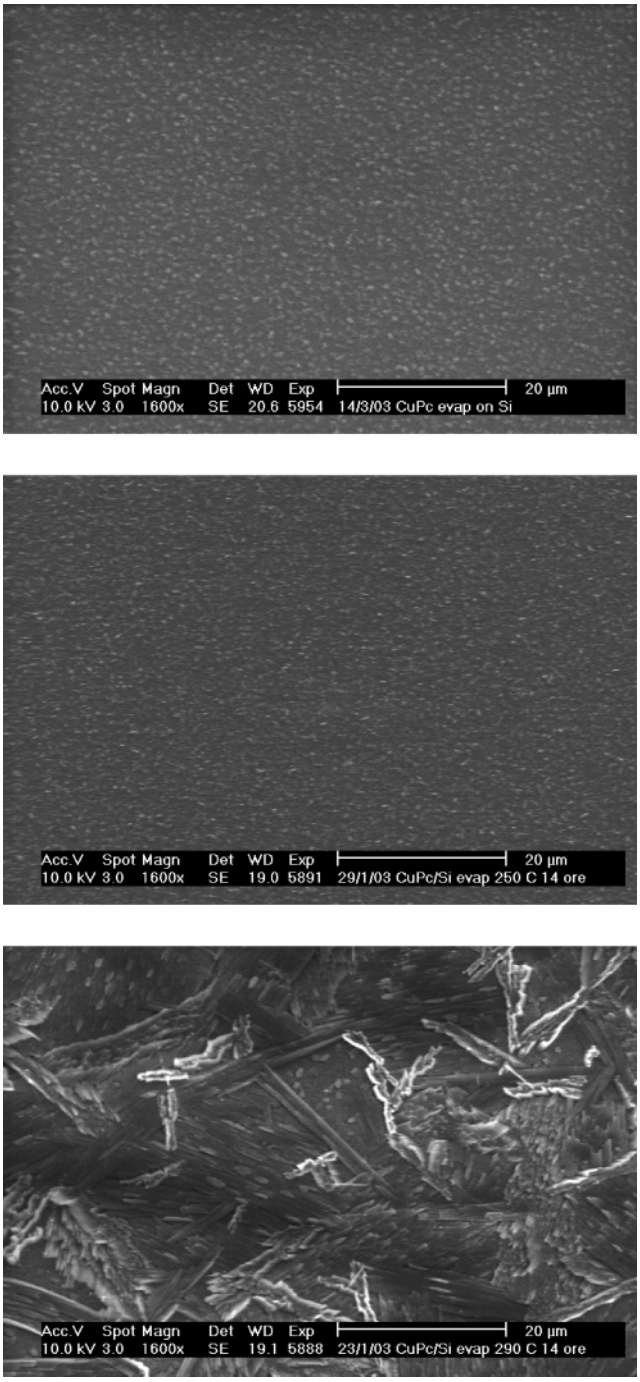

Figure 13. SEM micrographs of RTVE samples as-deposited (upper), treated at 250 °C (middle), and treated at 290 °C (lower).

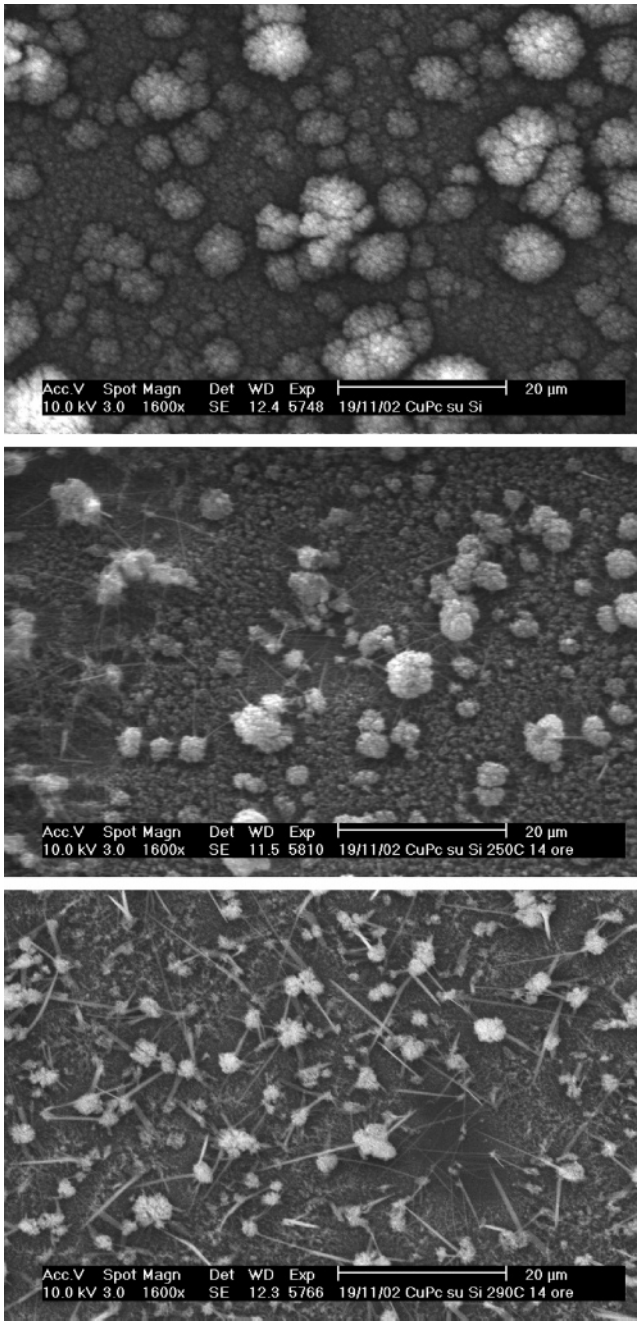

Figure 14. SEM micrographs of GDS samples as-deposited (upper), treated at 250 °C (middle), and treated at 290 °C (lower).

the VE samples. The splitting of the γ(C−H) peak in two components arises from the highly disordered structure of the as-deposited GDS film, characterized by a broad distribution of crystallite size and lattice parameter, and indicates that the thermal treatment determines a decrease of the structural disorder in the film. As a matter of fact, assuming that the α to β transformation depends on the crystallite size, the growth of β polymorph originates from the already present β crystallites and from the small α crystallites which undergo phase transformation. The growth of β polymorph is also confirmed by the slight increase of the IR peak at 780 cm^{-1} and by the appearance of two weak peaks at $d =$ 8.34 Å (−202) and $d = 7.06$ Å (002) in the XRD spectrum. On the other hand, the growth of α polymorph is due to the bigger α crystallites which do not change their crystalline structure. Finally, the possible residual strains present in the film are relaxed during the thermal treatment so that the distribution of lattice parameter narrows and the broadening of the γ(C−H) peaks of both polymorphs decreases. After the treatment at 290 °C, the GDS film consists of only β polymorph like the VE films.

UV−visible absorption measurements show that the spectrum of RTVE film treated at 250 °C does not exhibit differences as compared to that of the as-deposited film (see Supporting Information), to confirm that α to β transformation does not occur at this temperature. As to the GDS film, the main effect of the treatment at 250 °C is the growth of the absorption on the right side (higher wavelength) of the Q-band (Figure 12). On the contrary, the spectrum of the

GDS film treated at 290 °C has strongly changed: the total absorption is weaker and the Q-band shifts to higher wavelengths, with two peaks at 650 and 765 nm. The evolution of the spectral features of VE and GDS films corresponds well to their morphological changes. Figures 13 and 14 show the SEM images of all the samples. The treatment at 250 °C does not modify the surface morphology of the RTVE film while, after the treatment at 290 °C, the appearance of fibrous grains testifies to the α to β transformation.[35] In the GDS sample, the growth of needlelike structures, which are β crystallites,[10] is evident ever since the treatment at 250 °C (Figure 14). These needles become the prevailing structures on the film surface after the treatment at 290 °C.

4. Conclusions

Glow-discharge-induced sublimation (GDS) has been used to grow thin coatings of copper phthalocyanine (CuPc). The trend of the CuPc deposition rate is characterized by the appearance of pronounced spikes arising from the emission of molecular aggregates from the target surface. This very peculiar deposition rate together with the high deposition pressure gives rise to the growth of very disordered films featuring a much more porous structure than the evaporated films. The structure of the GDS films consists of a mixture of α and β crystallites, most likely with a broad distribution of size and lattice parameter. FT-IR analysis of the deposited films shows that they are mainly made of integer CuPc molecules, but an incorporation of a nonnegligible amount of molecular fragments is found at increasing deposition time. Nitrogen physisorption measurements point out that the GDS films feature a high porosity, characterized by a bimodal pore distribution peaked on micropores (2 nm about) and mesopores (>30 nm). The porous and rough morphology of the GDS films as compared to the VE samples makes these coatings particularly interesting for gas-sensing applications.

Heat treatments of the GDS films provoke the decrease of the structural disorder at 250 °C and the total transformation into the β phase at 290 °C. During the β polymorph growth, a needlelike structure develops on the film surface.

Finally, despite the many papers dealing with the structure of evaporated films, this study allowed to obtain also two important findings on the structure of these films, which were not clearly pointed out in the literature: (i) particular caution must be used when interpreting the FT-IR data of the CuPc films as related to their crystal structure, since the crystallite size proved to affect some IR features of the CuPc samples such as the position of the out-of-plane hydrogen-bending mode γ(C−H) peak, which is widely used for the identification of the CuPc polymorphs; (ii) the α to β transition temperature is related to the crystallite size: in particular, when the crystallite size is smaller than a threshold value, the α to β transformation is triggered; otherwise, the α crystallites preserve their structure. It has been shown here that small-grain-sized films (such as the LTVE films) undergo the α to β transition after only 14 h at 250 °C: the occurrence of this irreversible transformation can be a serious drawback to the application of these films to gas sensing, since a commercial sensing device must be working for months or years without significant changes.

Acknowledgment. This research was financially supported by the Fifth Commission of Istituto Nazionale di Fisica Nucleare (ASTHICO project).

Supporting Information Available: FT-IR spectrum of LTVE film heated at 250 °C for 14 h; UV−vis absorption spectrum of RTVE film heated at 250 °C for 14 h (PDF). This material is available free of charge via the Internet at http://pubs.acs.org.

CM0487122

(35) E, J.; Kim, S.; Lim, E.; Lee, K.; Cha, D.; Friedman, B. *Appl. Surf. Sci.* **2003**, *205*, 274.